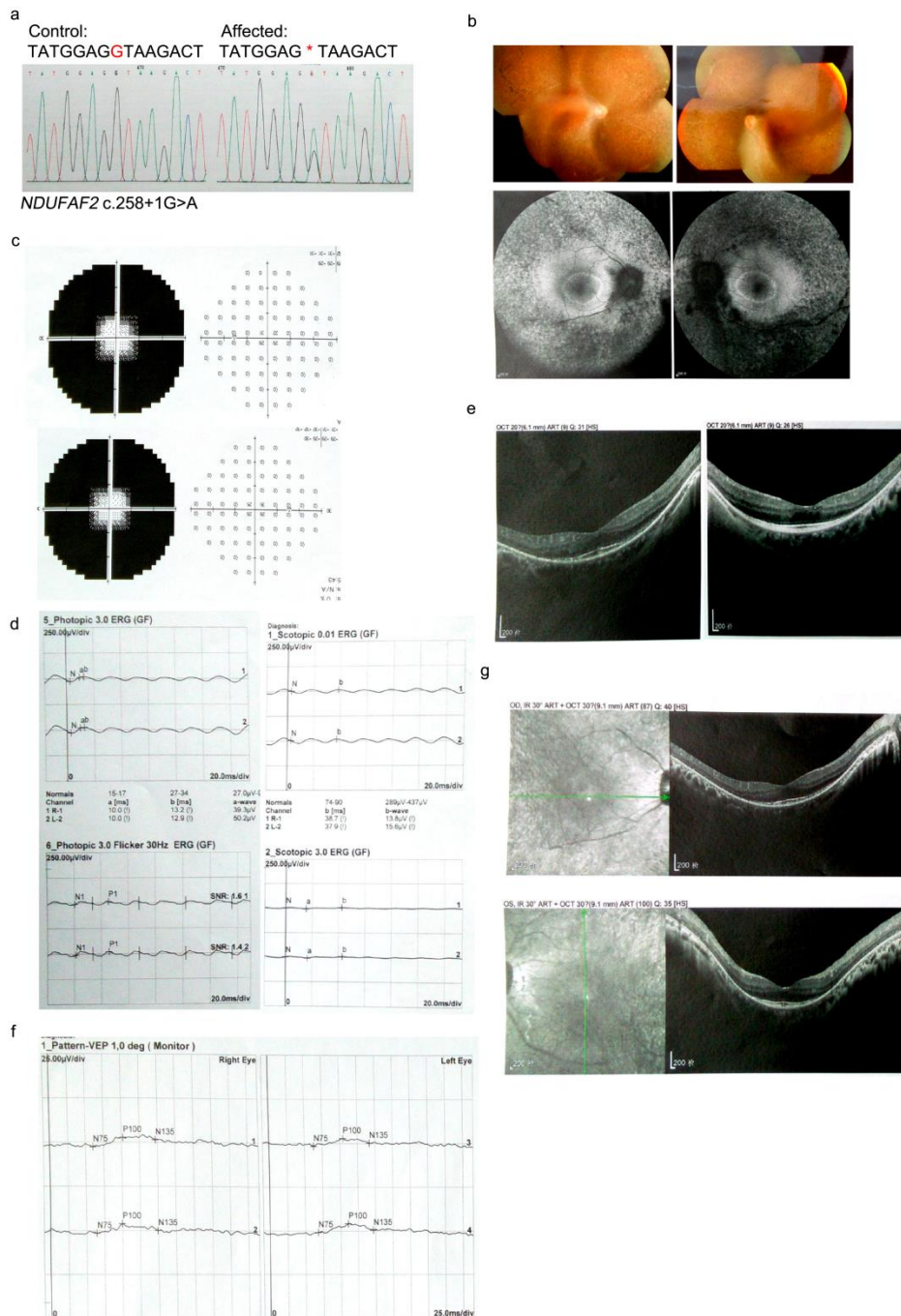


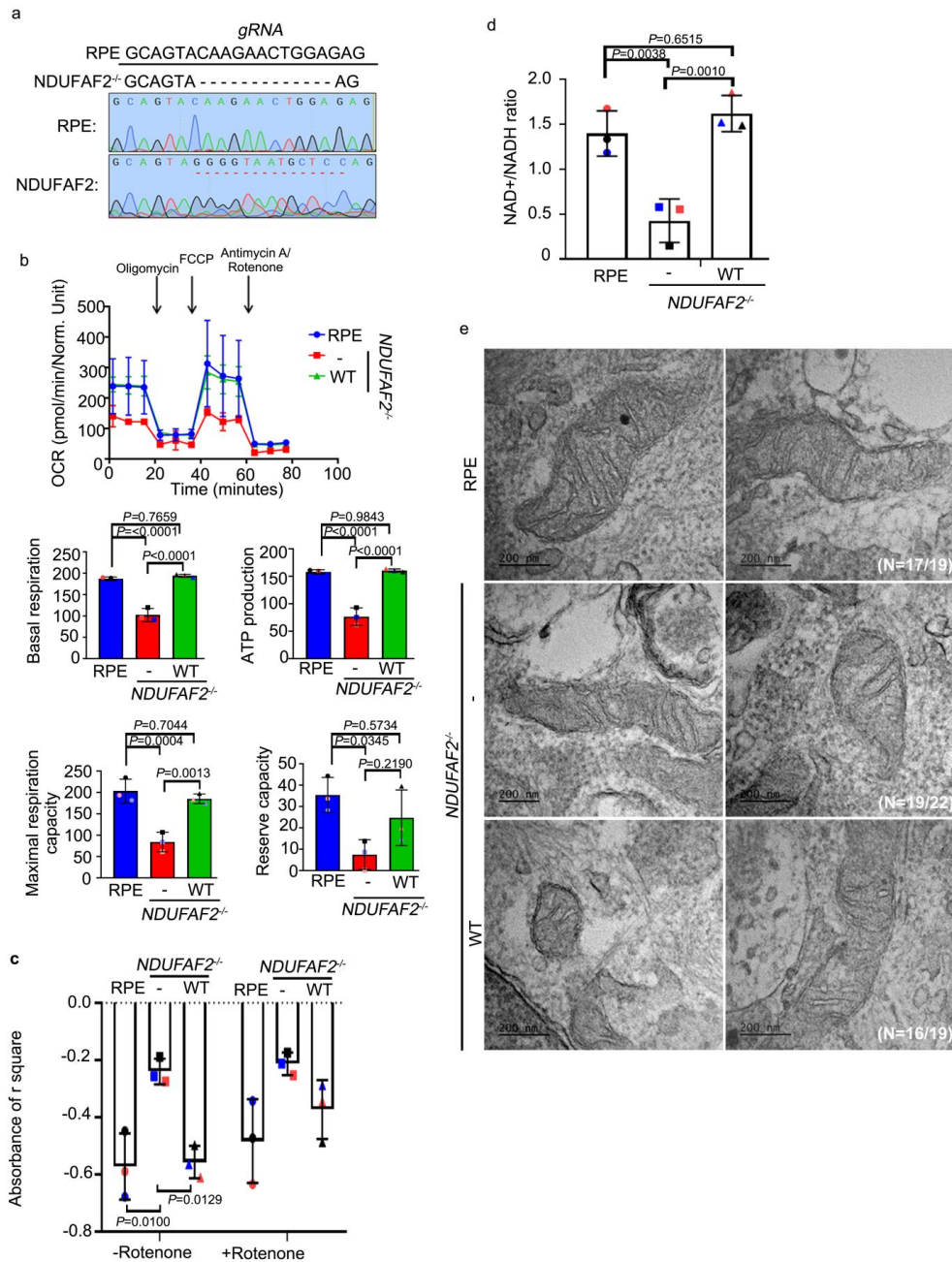
1 Supplemental Figure



2

3 **Supplemental Figure 1. NDUFAF2 mutation in a patient with bilateral retinal**
 4 **degeneration and optic nerve atrophy.** (a) A 28-yo woman presented with a novel
 5 NDUFAF2 mutation c.258+1 G>A (b) Color fundus photography of both eyes showing
 6 pale optic nerve, attenuated blood vessels, and pigmentary retinopathy. (c) Red-free
 7 fundus imaging showing bilateral diffuse pigmentary degeneration with residual
 8 bullseye lesion in central macula. (d) Humphrey visual field 24-2 demonstrating severe

9 constriction with preservation of central island in both eyes. (e) Photopic and scotopic
10 electroretinogram showing flat amplitude and decreased a- b- waves in both eyes. (f)
11 Ocular coherence tomography showing loss of photoreceptors and thinning of retinal
12 ganglion cell layer in both eyes. (g) Visual evoked potential (VEP) showing decreased
13 P100 amplitude in both eyes.
14



15

16 **Supplemental Figure 2. Loss of NDUFAF2 affects mitochondrial activity.** (a)

17 Editing sequencing outcomes in NDUFAF2^{-/-} cells. The upstream is the sequence of

18 RPE1 cells; the downstream is the sequence of two different NDUFAF2^{-/-} cells. (b)

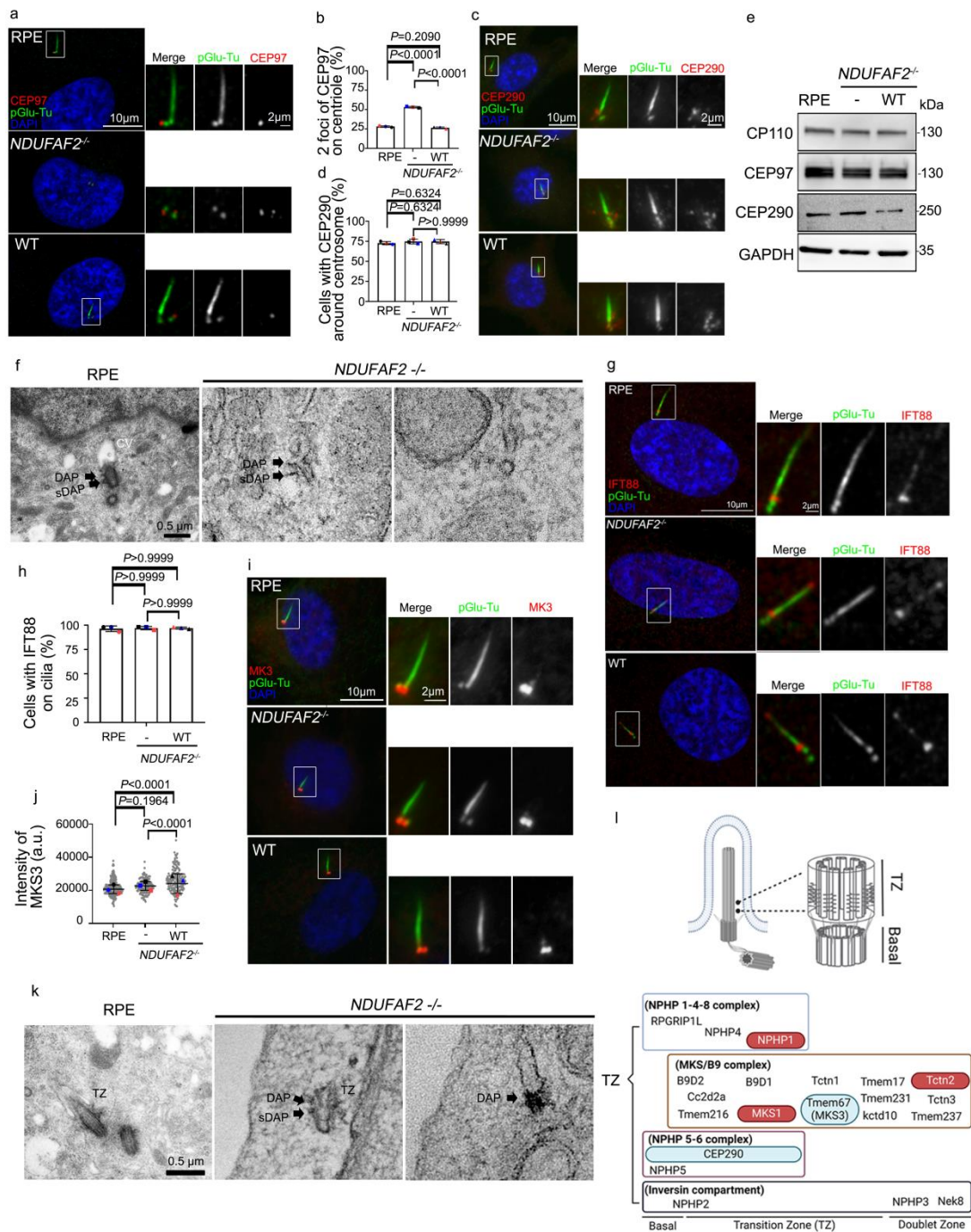
19 Mitochondrial activity in wild-type, NDUFAF2^{-/-}, and NDUFAF2^{WT}-re-expressing

20 RPE1 cells. The oxygen consumption rate was measured by Seahorse Analyzer. (c)

21 Catalytic enzyme activity of complex I in purified mitochondria of wild-type,

22 NDUFAF2^{-/-}, and NDUFAF2^{WT}-re-expressing RPE1 cells. (d) NAD⁺/NADH ratio in

23 wild-type, *NDUFAF2*^{-/-}, and *NDUFAF2*^{WT} -re-expressing RPE1 cells. (e) TEM
24 images of wild-type, *NDUFAF2*^{-/-}, and *NDUFAF2*^{WT} -re-expressing RPE1 cells
25 showing mitochondrial cristae. Bars in each graph represent mean ± SD. Exact *P*
26 values are indicated. ANOVA followed by a Tukey-Kramer multiple-comparison test.
27
28



29

30 **Supplemental Figure 3. Loss of NDUFAF2 in RPE cells results in transition zone**
 31 **defects.** (a) Immunofluorescent analysis of cells serum starved for 2 days. Cells
 32 stained with CEP97 (red) and pGlu-Tu (green) antibodies. DNA (DAPI, blue). Scale
 33 bars as indicated. (b) Graph shows the percentage of serum-starved cells with two
 34 CEP97 dots at the centrioles. > 150 cells analyzed for each independent experiment.
 35 (c) Immunofluorescent analysis of cells serum starved for 2 days. Cells stained with
 36 CEP290 (red) and pGlu-Tu (green) antibodies. DNA (DAPI, blue). Scale bars as

37 indicated. (d) Graph shows the percentage of serum-starved cells with CEP290 signals
38 around the centrioles. > 150 cells analyzed for each independent experiment. (e)
39 Western blot analysis was performed with antibodies against CP110, CEP97, CEP290
40 and GAPDH. (f) TEM images of wild-type and *NDUFAF2*^{-/-} RPE1 cells showing
41 centriole and ciliary vesicle. (g) Immunofluorescent analysis of cells serum starved
42 for 2 days. Cells stained with IFT88 (red) and pGlu-Tu (green) antibodies. DNA
43 (DAPI, blue). Scale bars as indicated. (h) Graph shows the percentage of
44 serum-starved cells with IFT88 signals on the cilium. > 150 cells analyzed for each
45 independent experiment. (i) Immunofluorescent analysis of cells serum starved for 2
46 days. Cells stained with MKS3 (red) and pGlu-Tu (green) antibodies. DNA (DAPI,
47 blue). Scale bars as indicated. (j) Quantification of MKS3 signal intensity at the
48 centrioles. > 100 cells analyzed for each independent experiment. (k) TEM images of
49 wild-type and *NDUFAF2*^{-/-} RPE1 cells showing centriole and transition zone (TZ). (l)
50 Schematic diagram showing the localization of transition zone. Red means affected
51 protein in *NDUFAF2*^{-/-} RPE cells and blue means unaffected protein in *NDUFAF2*^{-/-}
52 RPE cells. It is generated by BioRender. Bars in each graph represent mean ± SD.
53 Exact *P* values are indicated. ANOVA followed by a Tukey-Kramer
54 multiple-comparison test.

55

56

57

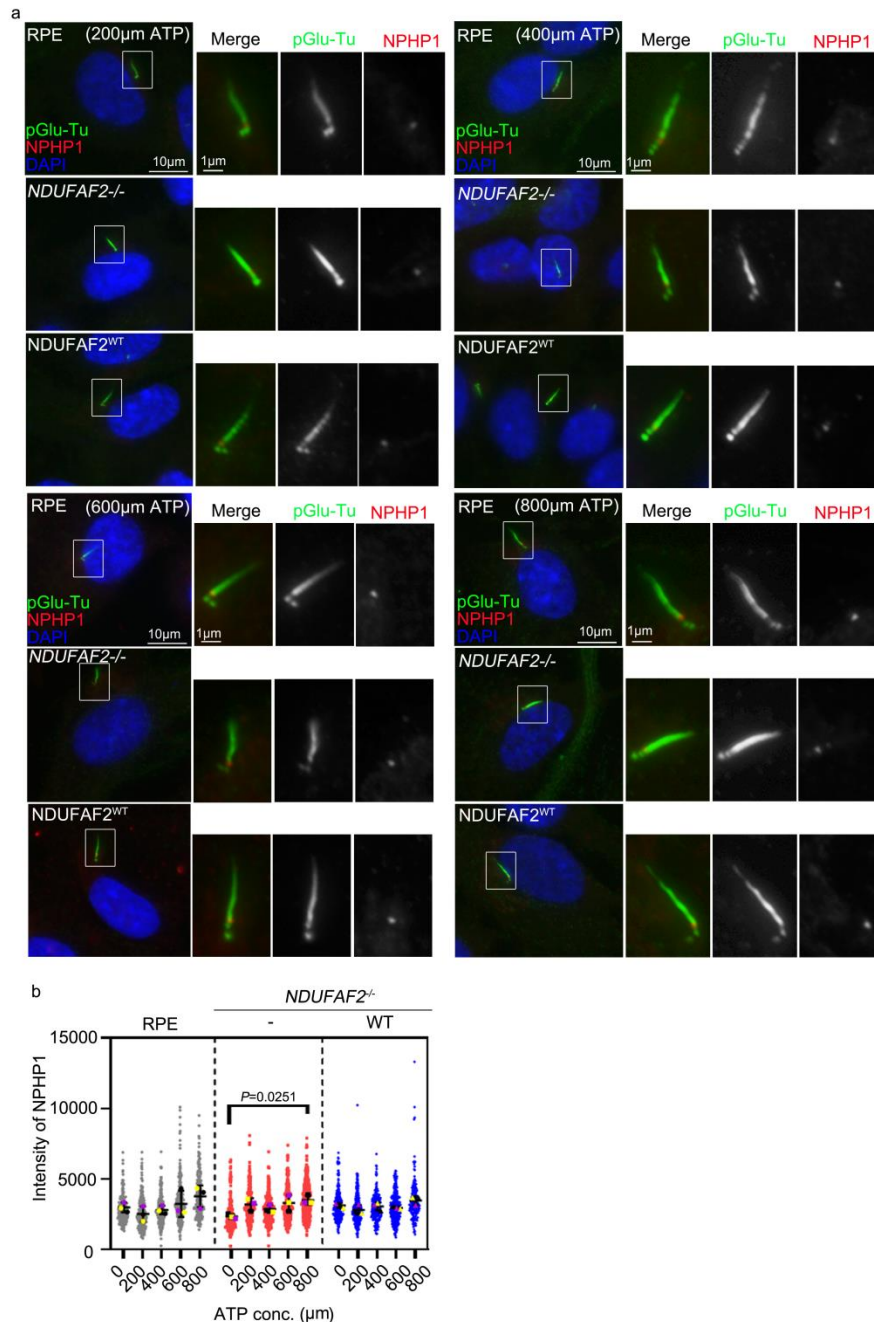
58

59

60

61

62



63

64 **Supplemental Figure 4. ATP promotes transition zone formation (a)**

65 Immunofluorescent analysis of cells serum starved for 2 days. Cells stained with

66 NPHP1 (red) and pGlu-Tu (green) antibodies. DNA (DAPI, blue). Scale bars as

67 indicated. (b) Quantification of the intensity of NPHP1 signals at the centrosomes. > 150

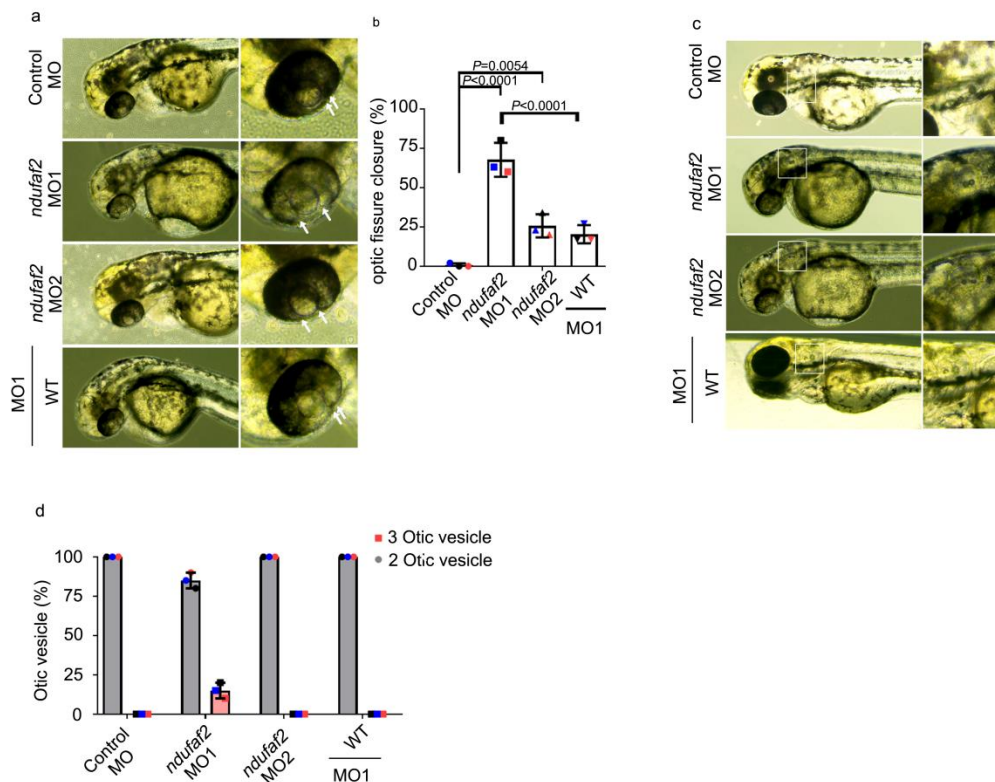
68 cells analyzed for each independent experiment. Bars in each graph represent mean ±

69 SD. Exact *P* values are indicated. ANOVA followed by a Tukey-Kramer

70 multiple-comparison test.

71

72



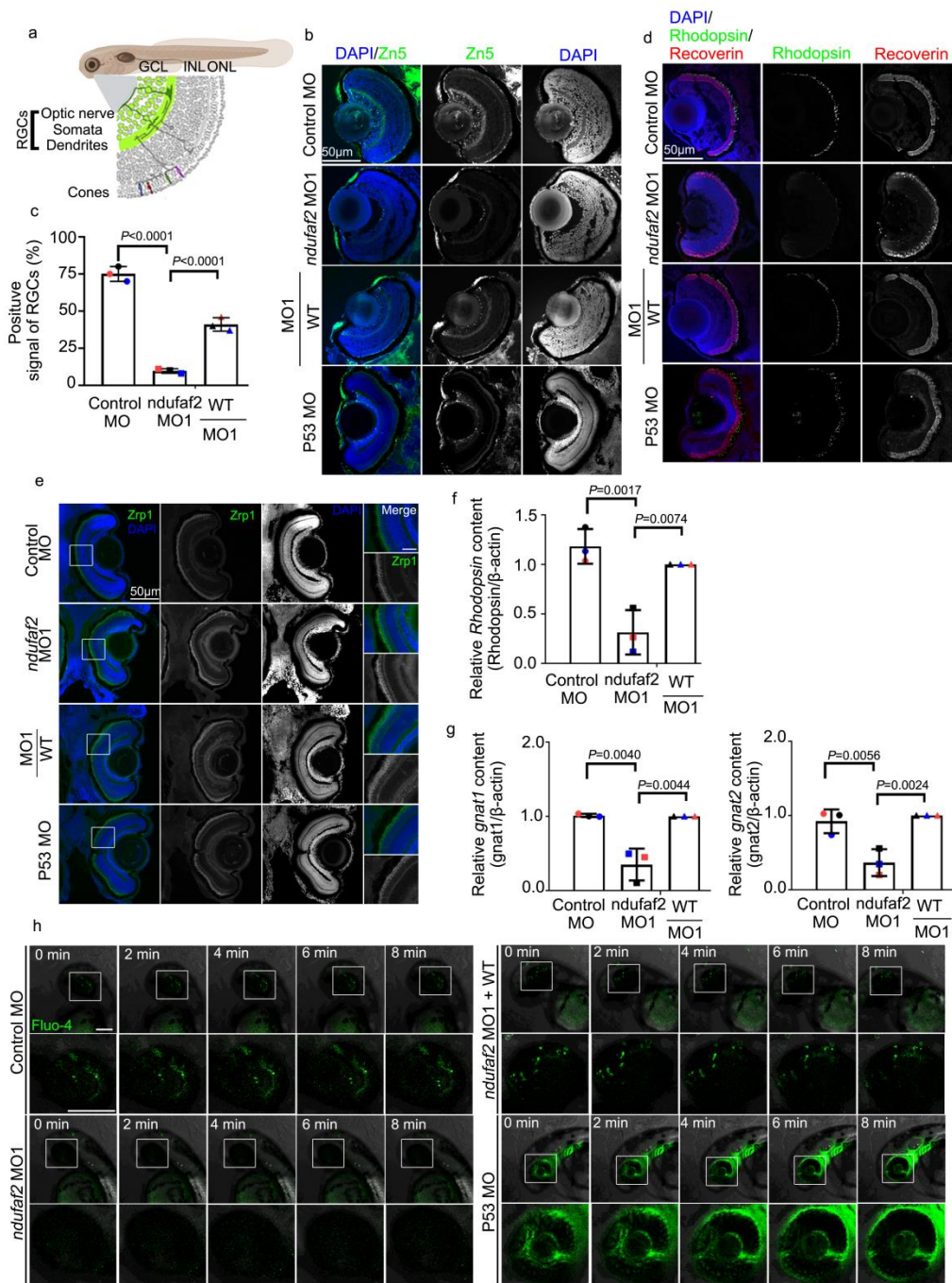
73

74 **Supplemental Figure 5. NDUF2 affects optic fissure closure but does not**
 75 **affect the number of otic vesicles.** (a) Transmitted light images of eyes in control
 76 MO, *ndufaf2* morpholino-injected zebrafish larvae and *NDUF2*^{WT} re-expressing in
 77 *ndufaf2* morpholino-injected zebrafish larvae at 3 dpf. Arrows indicate the margins of
 78 the optic fissure. (b) Quantification of optic fissure closure in control MO, *ndufaf2*
 79 morpholino-injected zebrafish larvae and *NDUF2*^{WT} re-expressing in *ndufaf2*
 80 morpholino-injected zebrafish larvae at 3 dpf. > 30 larvae analyzed for each
 81 independent experiment. (c) Transmitted light images of eyes in control MO, *ndufaf2*
 82 morpholino-injected zebrafish larvae, and *ndufaf2* morpholino-injected zebrafish
 83 larvae and *NDUF2*^{WT} re-expressing at 2 dpf. Arrows point to otic vesicle margins.
 84 (d) Quantification of optic fissure closure in control MO, *ndufaf2* morpholino-injected
 85 zebrafish larvae, and *ndufaf2* morpholino-injected zebrafish larvae and *NDUF2*^{WT}
 86 re-expressing at 2 dpf. > 30 larvae were analyzed for each independent experiment.
 87 Bars in each graph represent mean ± SD. Exact *P* values are indicated. ANOVA
 88 followed by a Tukey-Kramer multiple-comparison test.

89

90

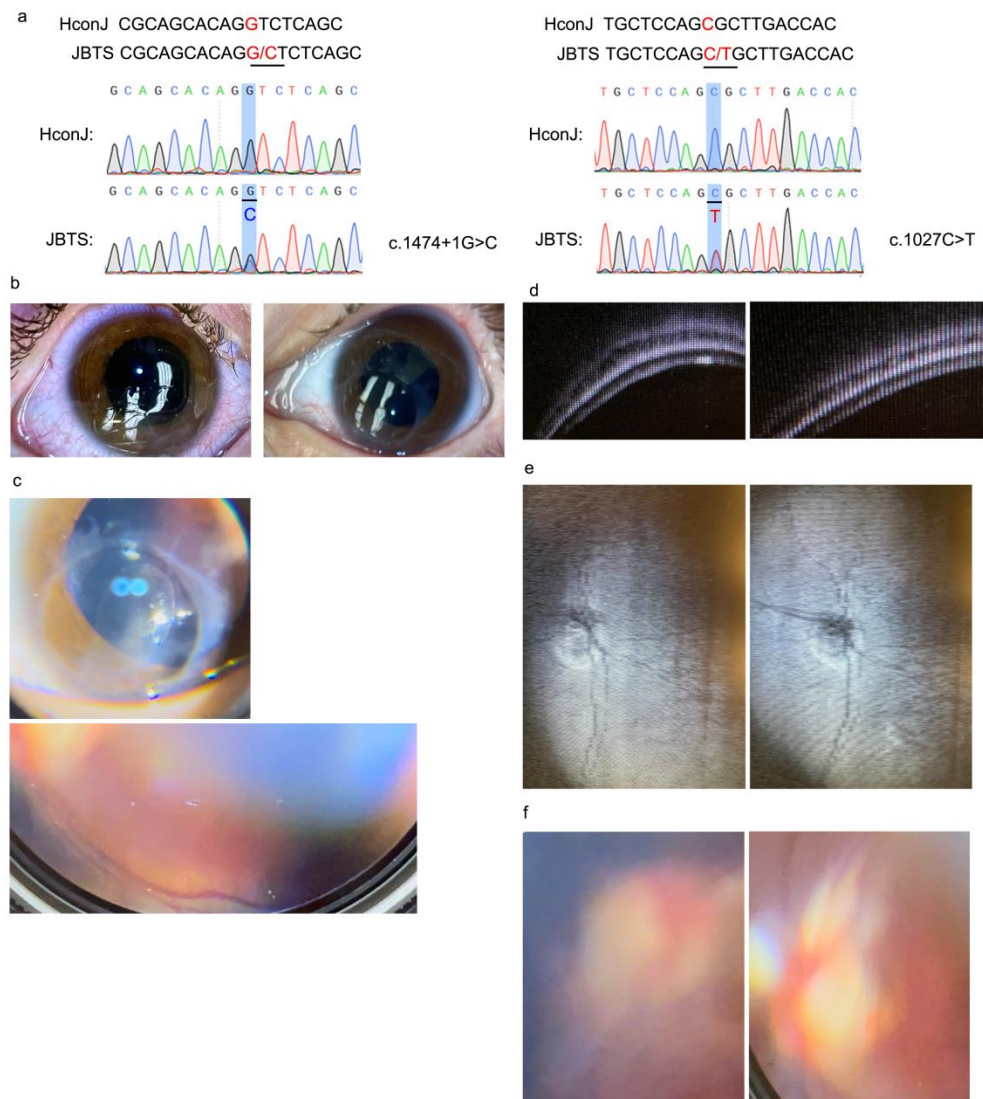
91



92

93 **Supplemental Figure 6. Photoreceptor dysfunction and degeneration in zebrafish**
 94 ***ndufaf2* morpholino-injected mutants.** (a) Schematic diagram showing
 95 photoreceptor structure in zebrafish. It is generated by BioRender. (b) Light
 96 microscopic images showing retinal ganglion cells (RGC) in zebrafish larvae at 5 dpf.
 97 Zebrafish larvae are stained with Zn5 (green), DNA is stained with DAPI (blue).
 98 Scale bars as indicated. (c) Quantification of RGC signals in the GCL region of
 99 zebrafish larvae at 5 dpf. 10 larvae analyzed for each independent experiment. (d)

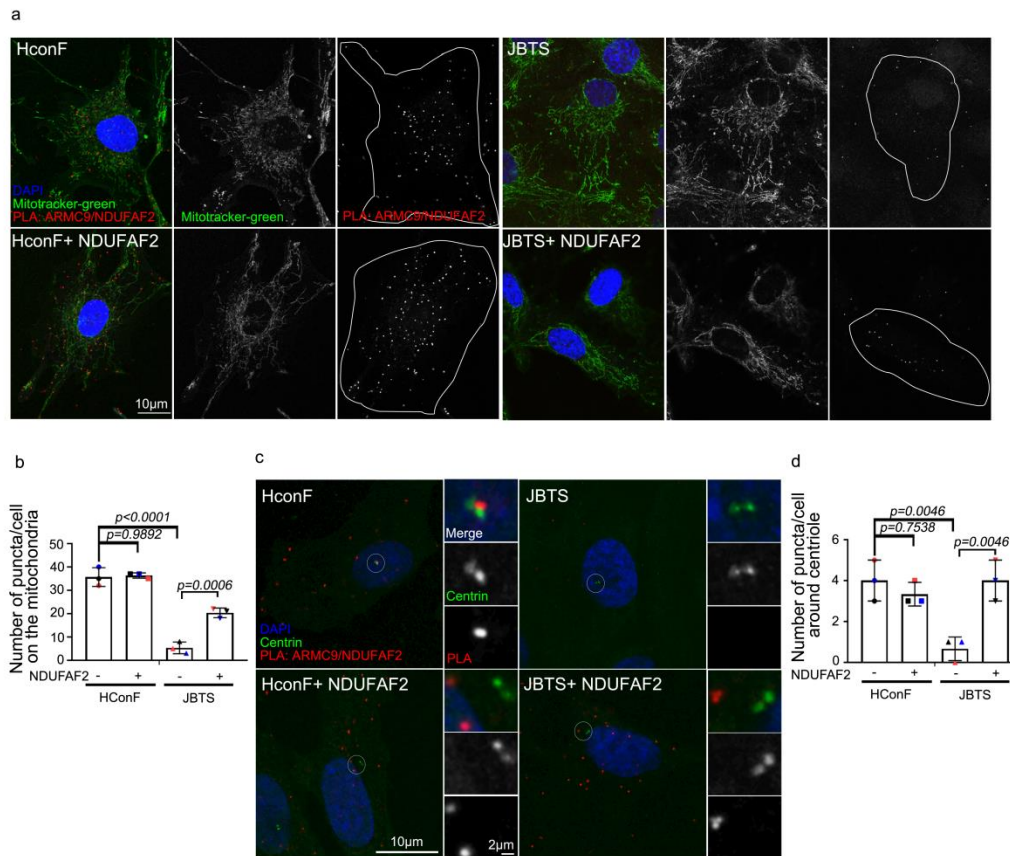
100 Light microscopic images showing photoreceptors in zebrafish larvae at 5 dpf.
101 Zebrafish larvae are stained with rhodopsin (green) and recoverin (red), DNA is
102 stained with DAPI (blue). Scale bars as indicated. (e) Light microscopic images
103 showing cone photoreceptor in zebrafish larvae at 5 dpf. Zebrafish larvae are stained
104 with Zrp1 (green), DNA is stained with DAPI (blue). Scale bars as indicated. (f)
105 Quantitative real-time PCR (RT-PCR) validation of rhodopsin in zebrafish larvae at 5
106 dpf. RT-PCR was repeated three times with different batches. Gene expression values
107 are normalized to β -actin. (g) Quantitative real-time PCR (RT-PCR) validation of
108 transducin (*gnat1* and *gnat2*) in zebrafish larvae at 5 dpf. RT-PCR was repeated three
109 times with different batches. Gene expression values are normalized to β -actin. (h)
110 Zebrafish larvae at 5 dpf were incubated at 28°C for 45 min with Fluo-4, calcium
111 indicator. Bars in the graph represent mean \pm SD. Exact *P* values are indicated.
112 ANOVA followed by a Tukey-Kramer multiple-comparison test.
113



114

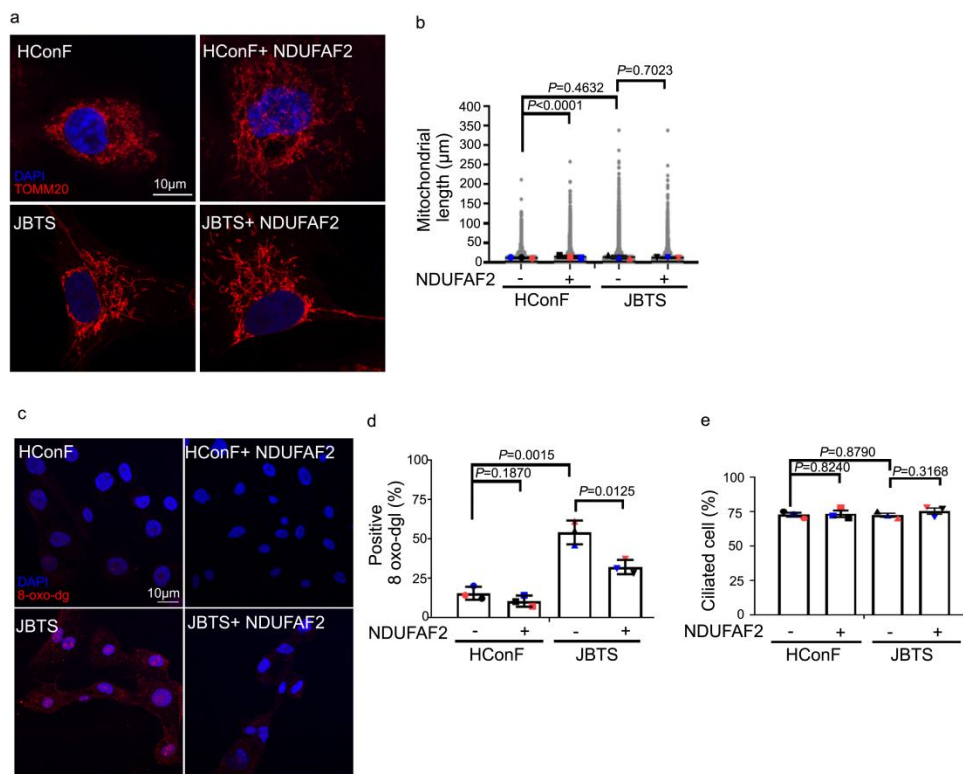
115 **Supplemental Figure 7. ARMC9 mutation-associated midbrain and retinal**
 116 **defects.** (a) The child carries ARMC9 mutations (case number UW349-3,
 117 c.1474+1G>C and c. 1027 C>T) (b) Anterior segment photos showing corneal
 118 exposure keratitis in right eye and inferior corneal transplant in left eye. (c) Retinal
 119 photograph of left eye showing early pigmentary retinal changes. (d) and (e) Ocular
 120 coherence tomography of right eye showing attenuated blood vessels. (f) Optic nerve

121 head photographs showing cupping of optic nerve in both eyes and myelinated optic
122 nerve in left eye.
123
124
125
126
127
128
129
130
131
132
133
134
135
136
137
138
139
140



141

142 **Supplemental Figure 8. The interaction between ARMC9 and NDAUFAF2 is**
 143 **decreased in JBTS patient-derived cells.** (a) Cells were incubated with
 144 mitochondrial marker in green and with anti-ARMC9 and anti-NDUFAF2 antibodies
 145 then examined using PLA probes in red. (b) Quantification of puncta on mitochondria
 146 in HConF cells, JBTS cells, and both cell lines overexpressing NDUFAF2.. (c) Cells
 147 were incubated with centriole marker in green and with anti-ARMC9 and
 148 anti-NDUFAF2 antibodies, then examined using PLA probes in red. (d)
 149 Quantification of puncta around centrioles in HConF cells, JBTS cells, and both cell
 150 lines overexpressing NDUFAF2. The bars in each graph represent mean \pm SD. Exact
 151 P values are indicated



152

153 **Supplemental Figure 9. NDUFAF2 rescues defective ciliogenesis in JBTS**

154 **patient-derived cells.** (a) Representative cells stained by immunofluorescence for

155 Mitotracker-red (red). Nuclei visualized with DAPI (blue). Scale bars 10 μm. (b)

156 Mitochondrial length measured by Mytoe of HConF cells, JBTS cells, and both cell

157 lines overexpressing NDUFAF2. > 100 cells measured. Bar line represents mean with

158 standard deviation (mean ± SD, Student's t test). (c) Representative cells stained by

159 immunofluorescence for 8-oxo-dg (red). Nuclei visualized with DAPI (blue). Scale

160 bars 10 μm. (d) Quantitation of 8-oxo-dg signal in individual cells. (e)

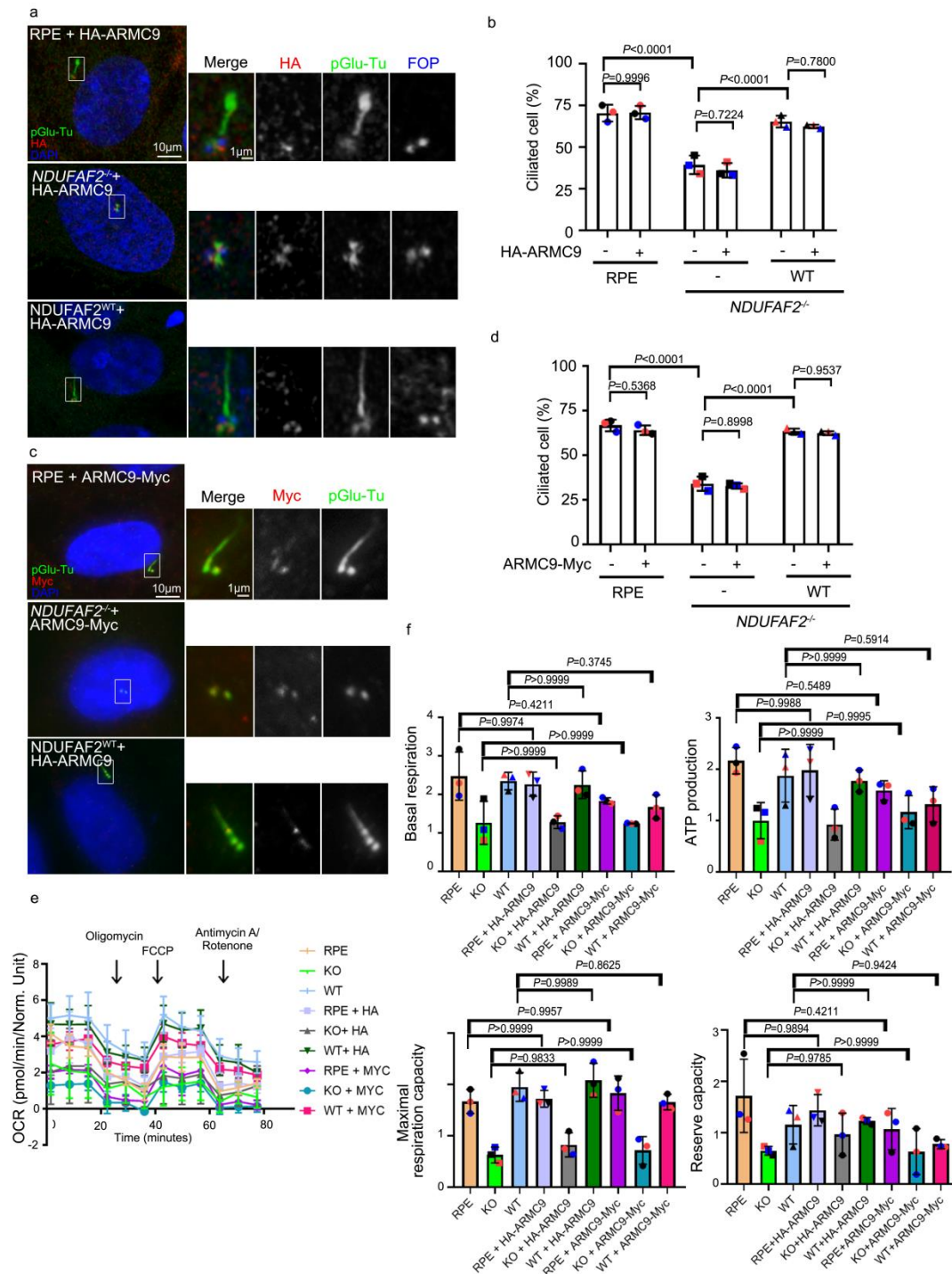
161 Immunostaining for polyglutamylated tubulin of cells serum starved for 2 days. The

162 percentage of ciliated cells is quantified. > 150 cells analyzed for each independent

163 experiment. Exact P values are indicated. ANOVA followed by a Tukey-Kramer

164 multiple-comparison test.

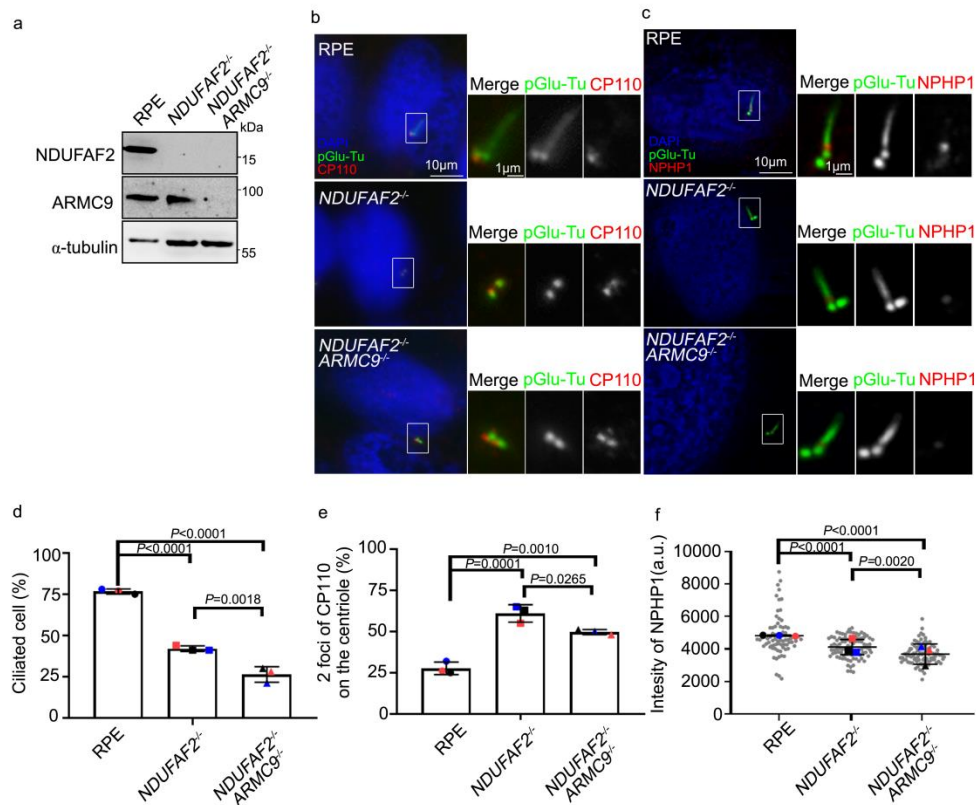
165



166

167 **Supplemental Figure 10. Overexpression of ARMC9 is not sufficient for cilia**
 168 **formation.** (a) Overexpression of HA tagged of N-terminal of ARMC9 into cells and
 169 immunofluorescent analysis of cells serum starved for 2 days. Cells stained with HA
 170 (red), pGlu-Tu (green) and FOP (blue) antibodies. DNA (DAPI, blue). Scale bars as
 171 indicated. (b) Percentage of ciliated cells after serum starving for 2 days. > 150 cells
 172 analyzed for each independent experiment. (c) Overexpression of Myc tagged of
 173 C-terminal of ARMC9 into cells and immunofluorescent analysis of cells serum

174 starved for 2 days. Cells stained with HA (red) and pGlu-Tu (green) antibodies. DNA
175 (DAPI, blue). Scale bars as indicated. (d) Percentage of ciliated cells after serum
176 starving for 2 days. > 150 cells analyzed for each independent experiment. (e) and (f)
177 Oxygen consumption rate of cells measured by Seahorse Analyzer. Exact *P* values are
178 indicated. ANOVA followed by a Tukey-Kramer multiple-comparison test.
179



180

181 **Supplemental Figure 11. ARMC9 is required for cilia formation** (a) Double

182 knockout ARMC9^{-/-} NDUFAF2^{-/-} cells. Western blot analysis performed with

183 antibodies against NDUFAF2, ARMC9, and α-tubulin. (b) Immunofluorescent

184 analysis of cells serum starved for 2 days. Cells stained with CP110 (red) and

185 pGlu-Tu (green) antibodies. DNA (DAPI, blue). Scale bars as indicated. (c)

186 Immunofluorescent analysis of cells serum starved for 2 days. Cells stained with

187 NPHP1 (red) and pGlu-Tu (green) antibodies. DNA (DAPI, blue). Scale bars as

188 indicated. (d) Percentage of ciliated cells after serum starving for 2 days. > 150 cells

189 analyzed for each independent experiment. (e) Graph shows the percentage of serum

190 starved cells with two CP110 dots at the centrioles. > 150 cells analyzed for each

191 independent experiment. (f) Quantification of the intensity of NPHP1 signals at the

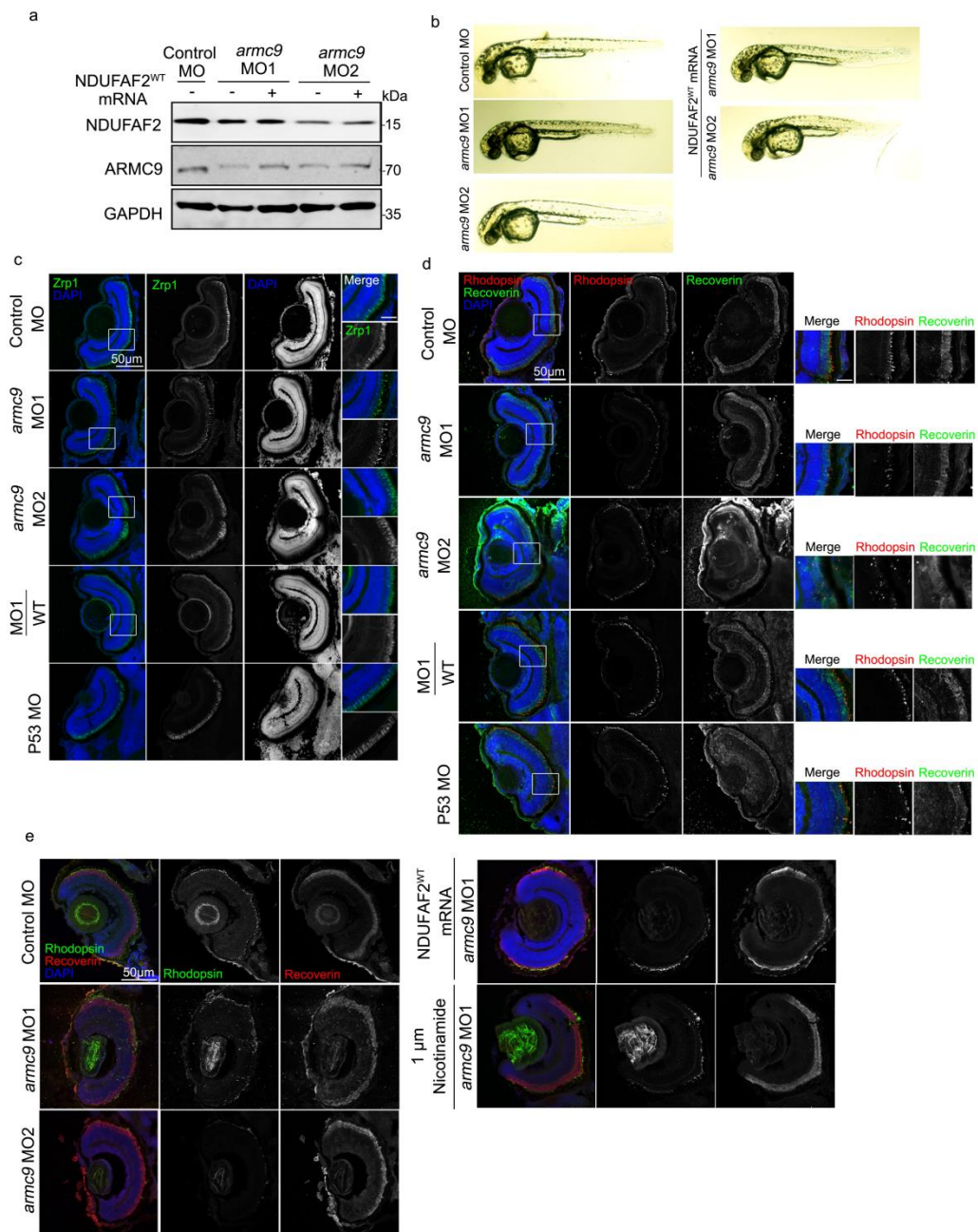
192 centrioles. > 50 cells analyzed for each independent experiment. The bars in each

193 graph represent mean ± SD. Exact P values are indicated. ANOVA followed by a

194 Tukey-Kramer multiple-comparison test.

195

196



197

198 **Supplemental Figure 12. NAD⁺ supplement rescues defective zebrafish**

199 **photoreceptor in vivo.** (a) Protein level of control MO, *armc9* morpholino-injected

200 embryos, Ndufaf2 mRNA and nicotinamide treatment in *armc9* morpholino-injected

201 embryos. Western blot analysis was performed with antibodies against ARMC9,

202 NDUFAF2 and GAPDH. (b) Transmitted light images of body shape in control MO,

203 *p53* and *armc9* morpholino-injected embryos. (c) Images of cone photoreceptors in

204 zebrafish larvae at 5 dpf. Zebrafish larvae stained for Zrp1 (green) and DNA stained

205 with DAPI (blue). Scale bars as indicated. Scale bar:50 μ m. Bars in each graph
206 represent mean \pm SD. (d) Images of photoreceptors in zebrafish larvae at 5 dpf.
207 Zebrafish larvae stained for rhodopsin (green) and recoverin (red), DNA stained with
208 DAPI (blue). (e) Images of photoreceptors in zebrafish larvae at 5 dpf with 1 μ m of
209 Nicotinamide and NDUFAF2^{WT} re-expressing in ndufaf2 morpholino-injected
210 zebrafish larvae. Zebrafish larvae stained for rhodopsin (green) and recoverin (red),
211 DNA stained with DAPI (blue). Scale bars as indicated. Scale bar (50 μ m. Bars in
212 each graph represent mean \pm SD.

213

214

215